Pesticide uptake and translocation in plants monitored in situ via laser ablation dielectric barrier discharge ionization mass spectrometry imaging

Author(s):
You, Xue; Lu, Qiao; Guan, Xiaokang; Xu, Zhouyi; Zenobi, Renato

Publication date:
2024-06-15

Permanent link:
https://doi.org/10.3929/ethz-b-000666231

Originally published in:
Sensors and Actuators B: Chemical 409, https://doi.org/10.1016/j.snb.2024.135532

Sensors & Actuators: B. Chemical 409 (2024) 135532

Contents lists available at ScienceDirect

Sensors and Actuators: B. Chemical

journal homepage: www.elsevier.com/locate/snb

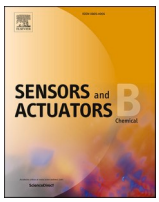

Pesticide uptake and translocation in plants monitored *in situ* via laser ablation dielectric barrier discharge ionization mass spectrometry imaging

Xue You [a], Qiao Lu [a,b], Xiaokang Guan [a], Zhouyi Xu [a], Renato Zenobi [a,c,*]

[a] Department of Chemistry and the MOE Key Laboratory of Spectrochemical Analysis & Instrumentation, College of Chemistry and Chemical Engineering, Xiamen University, Xiamen 361005, China
[b] Department of Laboratory Medicine, Taihe Hospital, Hubei University of Medicine, Shiyan 442000, China
[c] Department of Chemistry and Applied Biosciences, ETH Zurich, Zurich CH-8093, Switzerland

ARTICLE INFO

Keywords:
Laser ablation
Dielectric barrier discharge ionization
Atmospheric pressure mass spectrometry imaging
Mechanisms of pesticides uptake and translocation

ABSTRACT

For reducing pesticide usage and enhancing the effectiveness of pest control, it is necessary to elucidate the mechanisms of pesticide uptake and translocation in plants. Here, atmospheric pressure laser ablation dielectric barrier discharge ionization mass spectrometry imaging (LA-DBDI-MSI) was used to for *in-situ* monitoring of pesticide uptake and translocation in plants with a spatial resolution of 25 μm, and only requiring minimal or no sample preparation. Roots and leaves of tomato plants that had been exposed to a systemic pesticide, difenoconazole, were studied. From MSI data of tomato leaves, we found that difenoconazole was mainly distributed in the leaf veins after 6 days of pesticide exposure, but distributed throughout the leaf after 10 days of pesticide exposure. Endogenous substances are mainly distributed in the mesophyll, but are not present in the veins. This study clarifies the uptake and translocation mechanism of pesticides in plants, which is of great significance for reducing the dosage of pesticides and improving the effect of plant disease control.

1. Introduction

The development of modern agriculture is inseparable from the use of fertilizers and pesticides. Pesticides are widely used for pest control [1], weeding [2], regulating plant growth [3], etc. However, the heavy use of pesticides has negative impacts on the environment [4–6] and on public health [7,8] that cannot be ignored. The controversy on the use of pesticides has also received continuous public attention. One uncomforatble fact is that more than 90% of pesticides are lost during application, due to losses during spraying, wash-off by rain, environmental degradation and other factors. Moreover, plants absorb pesticides so inefficiently that the amounts of pesticides that enter the plants is very small. In the end, very little of the pesticides applied (less than 0.1%) reach their target [9], and more than 99.9% of them remain in the environment. Large amounts of pesticide residues thus contaminate soil, water and the atmosphere, aggravating the resistance of pathogens and pests to pesticides, reducing soil biodiversity, leading to bioaccumulation of pesticides, and posing risks to wild bees among other negative effects [10,11]. Therefore, it is particularly important to improve the utilization of pesticides.

An attractive strategy to enhance the uptake efficiency of pesticides by crops and the targeting ability of pesticides is to develop carrier-mediated modified pesticides [12,13]. Moreover, research on the absorption, translocation, metabolism, and distribution of pesticides can provide technical guidance for the development and use of pesticides, which is of great significance for reducing pesticide dosage and improving the utilization of pesticide [14–19]. Pesticide absorption and translocation behaviors have been widely studied [20–22]. Pesticides can be absorbed into plants via the roots, stems and leaves, and be transported through the vascular system, xylem and phloem [23,24]. Gas Chromatography-Mass Spectrometry (GC-MS) and Liquid Chromatography Mass Spectrometry (LC-MS) are widely used in investigating the absorption, translocation, metabolism and distribution of pesticides in plants [25–28]. And imaging techniques, such as fluorescence spectroscopy [17], imaging via isotopically labeled tracers [20], and surface-enhanced Raman spectroscopy (SERS) [29] have been used to monitor the dynamic distribution of pesticide molecules and reveal the mechanisms of pesticide absorption and translocation in plants. However, these visualization methods require additional processing (e.g., fluorescence labeling, isotope labeling, preparation of nanoparticles).

* Corresponding author at: Department of Chemistry and the MOE Key Laboratory of Spectrochemical Analysis & Instrumentation, College of Chemistry and Chemical Engineering, Xiamen University, Xiamen 361005, China.
E-mail address: zenobi@org.chem.ethz.ch (R. Zenobi).

https://doi.org/10.1016/j.snb.2024.135532
Received 29 November 2023; Received in revised form 8 February 2024; Accepted 20 February 2024
Available online 22 February 2024

These treatments are also time-consuming and labor-intensive, and tagging of pesticides may interfere with the absorption and metabolism of the pesticide molecule itself in plants.

Mass spectrometry imaging (MSI) cannot only realize label-free, *in-situ*, nonspecific detection, but also visualize the distribution of a wide variety of compound classes, incluging amino acids, nucleic acids and proteins, small molecules, etc. Therefore, MSI is widely used in drug distribution studies [30], histopathology [31], plant metabolomics [32], and other fields. For example, matrix-assisted laser desorption/ionization (MALDI) MSI was performed on root sections for revealing metabolomics of two Paeonia species [33]. However, the matrix peaks were found to interfere with the metabolite signals in the low *m/z* range, and moreover, MALDI methods require complex sample preparation. Metabolic imaging at the single-cell level was carried out using secondary ion mass spectrometry (SIMS) imaging [34]. Although these technologies feature both high lateral resolution and high mass-resolving power, they require high vacuum, which is incompatible with biological specimens.

Recently, the ambient MS methodology has witnessed significant developments. Using this technique, the sample can be held at ambient temperature and pressure, which is very suitable for biological samples. Cooks *et al.* first proposed the use of desorption electrospray ionization (DESI) [35] for mass spectrometric sampling under ambient conditions. Since then, many other ambient MS methods, including laser-based atmospheric pressure MSI technologies have emerged. Spengler *et al.* reported on AP-MALDI MSI to locate the distribution of lipids, metabolites and peptides in paramecium with a lateral resolution of only 1.4 μm [36]. Stopka *et al.* used fiber-based laser ablation electrospray ionization (f-LAESI) MS to image multiple cells to get insight into cellular heterogeneity [37]. In addition, AP nanoparticle- and plasma-assisted laser desorption ionization (AP-nanoPALDI) MSI was performed on tissue slices to obtain position information for metabolites with a lateral resolution of 2.9 μm [38]. These technologies combine the high-precision sampling of lasers with the simplicity and convenience of atmospheric pressure mass spectrometry.

In this paper, a laser ablation dielectric barrier discharge ionization (LA-DBDI) MSI approach [39] is introduced to investigate the pesticide uptake and translocation behavior in plants. Difenoconazole, a widely used pesticide, was applied to tomato plants via either the roots or leaves, and its translocation to the entire plant through vascular tissues was followed with the LA-DBDI MSI approach. After several days, difenoconazole could be detected in parts of the tomato plants that had not been in contact with the pesticide directly.

2. Materials and methods

2.1. Materials

Difenoconazole (1-((2-(2-chloro-4-(4-chlorophenoxy) phenyl)−4-methyl-1, pesticide stock solution) was purchased from Hebei Zhongbao Lvnong Crop Technology Co., Ltd. Difenoconazole is a high-efficiency, broad-spectrum variety of a triazole fungicide with strong systemicity, and has excellent protective and therapeutic effect for many plant species against a variety of fungal diseases. Tomato seedlings and horticultural nutrient soil were purchased from Shandong Shouhe Seed Industry Co., Ltd. (Shandong, China). Ethanol (C_2H_5OH, analysis grade,) was purchased from Sinopharm Group Chemical Reagent Co., Ltd. (Shanghai, China). All aqueous solutions were prepared using ultrapure water (18.2 MΩ·cm) from a Milli-Q ultrapure water system (Millipore, MA, U.S.A.).

2.2. Laser ablation post-ionization source

The second harmonic (532 nm) of a Nd:YAG laser (Nano SG60–30, Litron Inc., Rugby, Warwickshire, England) with a repetition rate of 10 Hz, a pulse duration of 5 ns, and a beam diameter of 4 mm was used for ablation. The laser beam was first reflected by a set of mirrors, and finally focused on the sample target by an air-spaced doublet lens (ACA254–060–532, Thorlabs Inc. Newton, NJ, U.S.A.). The focused laser beam ablated the sample, forming an ablation plume. The ablated material was transported into the post-ionization source due to the pressure difference between the atmospheric environment and the vacuum in the mass spectrometer.

A home-made DBDI source in the "active sampling capillary" configuration [40] was used as the post-ionization source, as described in detail in our earlier publication [39]. It was coupled to the MS inlet via a Teflon connection tube. Briefly, an alternating high voltage (40 kHz, ~3.5 kV) was applied to the two electrodes, which were separated by a dielectric (a glass capillary with I.D. 1.15 mm and O.D. 1.55 mm). The constant underpressure in the instrument ensured a fixed flow rate of air (0.9 L/min) through the capillary. The plasma was maintained at the position where the inner and outer electrodes overlapped, and gaseous molecules in the ablation plume are ionized as they pass through the plasma. The DBDI source has the advantage of being very simple to construct, and because of the "active sampling capillary" configuration, no additional carrier gas (such as nitrogen or argon) was needed, which also made the generated plasma more stable. The ion transmission efficiency was close to 100%, and it can be interfaced to any ambient inlet MS instrument.

In addition, a CCD camera was used to monitor the distance between the sample surface and the DBDI inlet. The energy of the ablation laser was measured by an energy measurement system (Ophir Optronics Solutions Ltd. Jerusalem, Israel), containing an energy meter (model VEGA) and a sensor head (model PE25BF-C).

2.3. LA-DBDI-MSI apparatus and data analyses

The LA-DBDI-MSI instrument is shown in Fig. 1. A two-dimensional linear positioner (SLC-1720 s, SmarAct GmbH, Oldenburg, Germany) with nanometer precision was used for sample translation. Samples were fixed on the sample plate with double-sided adhesive tape. A self-compiled program written in LabVIEW 2015 (National Instruments, Austin, TX, U.S.A.) and a homebuilt time delay generator were used to synchronize the movement of sample plate with the triggering of laser pulses. Here, the sample was scanned with a defined step size of 25 μm; each position was irradiated with only one laser shot, and a mass spectrum was obtained after each laser shot. A quadrupole/time-of-flight mass spectrometry (Q-TOF MS) system (API-TOF, TOFWERK AG., Thun, Switzerland) was used in positive ion mode and in the 7−500 *m/z* mass range. The capillary voltage, capillary temperature, and TOF extraction rate were set to 0 V, 200 °C, and 16 kHz, respectively.

Raw data were post-processed first via Tofware version 3.2.1 software (TOFWERK AG., Thun, Switzerland) and the mass spectra were evaluated with OriginPro 9.0 (OriginLab, Northampton, MA, U.S.A.). By reconstructing the XY coordinates and combining the MS signal intensities of the *m/z* of interest, the 3D data matrices obtained were used to produce MSI by a commercial scientific graphics software (Surfer 12, Golden Software LLC, Golden, CO, USA).

2.4. Imaging performance

LA-DBDI MSI is a laser-based atmospheric pressure mass spectrometry imaging technology. The lateral resolution of MSI is closely related to the size of the laser sampling crater. However, due to the limited laser ablation efficiency, ionization and transmission efficiency of the analyte, and detection efficiency of the MS, the imaging resolution cannot be improved arbitrarily by simply reducing the size of the sampling crater. In our experiment, we set the step size of the sample platform to 25 μm, and the laser sampling crater diameter obtained was also 25 μm, which is therefore defined as the imaging resolution. We set the laser frequency to 10 Hz and the image size to 6 × 6 mm^2. Therefore, the movement time of each line on the X axis is 24 s (X-axis size / (step×laser

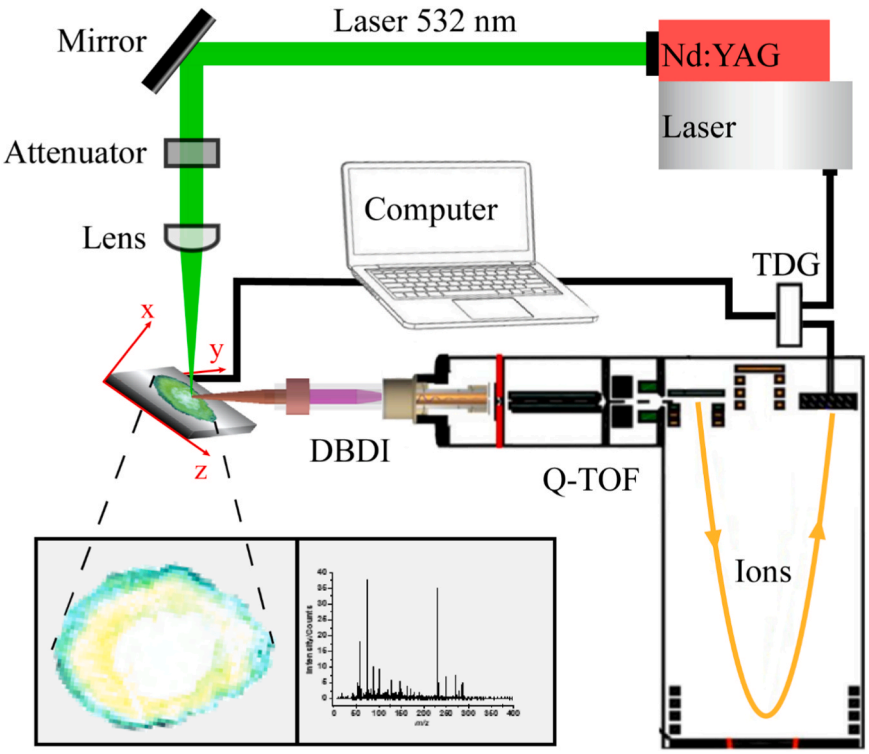

Fig. 1. Schematic diagram of the LA-DBDI-MSI system. DBDI = Dielectric barrier discharge ionization source, Q-TOF MS = Quadrupole time-of-flight mass spectrometer, TDG = Time delay generator, Nd:YAG = Nd:YAG laser.

frequency)), and the time interval from one line to the next is 7 s (the platform returns to the initial position of the X-axis and moves one step in the Y direction). The total time to scan a line is 31 s, and the total time required to scan the imaging area is 31 s×240 (Y-axis size / step) =7440 s (approximately 2 hours). The total time required for imaging is thus reasonably short. At the same time, because the imaging operates under atmospheric pressure conditions, the sample pretreatment requirements are low, and sample exchange is convenient. For plant

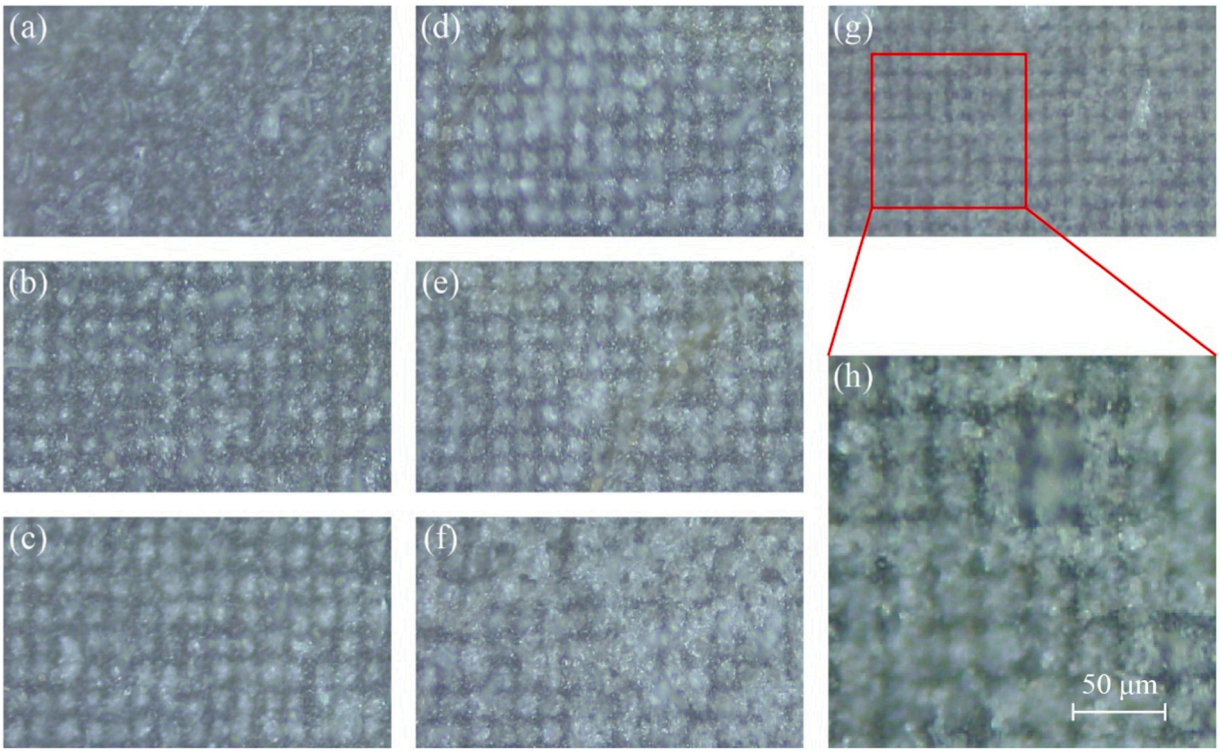

Fig. 2. (a-f) Optical microscopy images of craters on a tomato leaf after LA, using a step size of 50 μm, laser power of ~10 μJ, ~20 μJ, ~30 μJ, ~40 μJ, ~60 μJ, ~80 μJ. (g) with step width of 25 μm, laser power of ~40 μJ. (h) Zoomed view of part of the image shown in (g).

samples, we only need to perform simple sample pre-preparation steps such as washing, slicing, drying and flatting. Since no other chemical reagents are used, chemical pollution is avoided and the integrity of biological samples is preserved.

2.5. Evaluation of the lateral resolution

The LA-DBDI-MSI system was composed of several parts, a time delay generator, a laser ablation system, a sample displacement platform, a real-time sample observation system, the mass spectrometer, and an imaging data processing system.

To determine the lateral resolution of the LA-DBDI-MSI system, we first studied the relationship between laser energy and craters size created by the laser pulses. Flat and dry tomato leaves were selected for laser scanning, with typical operating parameters of the LA-DBDI-MSI system: a step size of 50 μm, laser frequency of 10 Hz, and a range of laser powers (~10 μJ, ~20 μJ, ~30 μJ, ~40 μJ, ~60 μJ, ~80 μJ). After laser ablation, the area scanned was evaluated under a laser scanning microscope. Fig. 2(a)-(f) shows the laser ablation craters on the surface of tomato leaves generated by different laser energies. With the same laser energy, the size of each ablation crater was uniform and a regular spacing between the craters in the scanning area was apparent. The off-white spots indicate that the laser successfully created ablation craters on the tomato leaves surface. With increasing laser energy, the size of the laser ablation craters gradually became larger, and the spacing between the craters decreased. When the laser energy was 80 μJ the craters overlapped, which means that the crater diameter was larger than 50 μm. We thus changed the step width to 25 μm and the laser energy was set at ~40 μJ. Under these conditions, the laser ablation craters could still be clearly distinguished. A lateral resolution of 25 μm is perfectly suitable for the MSI requirements of our selected plant samples: in the case of a lateral resolution of 25 μm, each row (6 mm) of MSI has 240 pixels, enough to render the tissue structure on the plant leaves. Taking into account the time required for imaging (the time of MSI required for 6 × 6 mm area is ~2 h), the shorter the time taken for a single MSI, the higher the MSI throughput. Therefore, the lateral resolution of the MSI system was set to 25 μm, and these experimental settings were selected for our subsequent studies.

2.6. Plant culture and sample preparation

For the case where pesticides were applied to the roots, tomato seedlings at the same growth stage were transferred to individual beakers containing 50 cm^3 horticultural nutrient soil. Each beaker contained two tomato seedlings, and was covered with aluminum foil to avoid exposing the roots to sunlight. Water was poured into each beaker every 12 h to keep the soil moist. The soil pH was adjusted to 6.5 with 2 (N-morpholino)ethanesulfonic acid and NaOH buffer. After three days of cultivation, a total of 10 mL of difenoconazole solution (100 ppm) was prepared and added to horticultural nutrient soil for absorption via the roots. This was repeated five times with 12-hour intervals each time.

For the case where pesticide was applied to the leaves, the same protocol as above was used for cultivating the plants, but instead of adding pesticides solution to the soil, the pesticide solution was brushed directly onto the leaves. A 0.1% pesticide solution was brushed onto the three leaves at the bottom of the tomato seedling five times, air-dried after each application, and absorbent paper was placed under the leaves to prevent the pesticide from dripping into the horticultural nutrient soil. That process was performed once a day for a total of two days. For these experiments, each beaker contained only one tomato seedling with six leaves. The application of the pesticide on the leafs was done without the use of a standard formulation. This may have some effect on the distribution and uptake of the compound, however, the detection of the pesticide in the leafs is just as effective, and not at all affected by the way of application. Leaves were removed from tomato seedlings by surgical scissors, then the harvested leaves were rinsed with ultrapure water and placed flat onto a glass slide. The excess water droplets on the leaves were absorbed by lint-free paper. Finally, tomato leaves were air-dried and flattened between two clean glass slides.

3. Results and discussion

3.1. Measurement of MS signal from difenoconazole on tomato leaf surfaces

As shown in Fig. 3(a), mass spectral signals originating from difenoconazole were clearly observed on tomato leaf surfaces after 10 days of applying difenoconazole on the roots. The signal at $m/z = 406$ was assigned to protonated difenoconazole. With either the laser or the DBDI turned off, the $m/z = 406$ peak was not detected. With solely the DBDI operating, only background signals from the lab air, such as plasticizers and other pollutatns, were observed, some of them ($m/z = 231$, 249) with substantial intensity, because they ionize easily with DBDI. With both the laser and the DBDI turned on (i.e., with difenoconazole present on the leaves), the characteristic MS signal of difenoconazole at $m/z = 406$ and other mass spectral signals related to endogenous substances in tomato leaves appear. When performing a control experiment on a blank sample, the parent ion of difenoconazole disappeared as expected. Therefore, the above results indicated that difenoconazole present on the surface of tomato leaves was ablated by the laser, ionized by DBDI source and finally successfully detected by mass spectrometry. The soil was analyzed after the test and difenoconazole molecules were detected, demonstrating the stability of the tested compounds. No possible degradation products of difenoconazole were found. In Fig. 3(c), no fragment peaks of difenoconazole were observed, which is attributed to the relatively soft ionization ability of the low-temperature plasma generated by the DBDI source [41].

In order to evaluate the ability of the LA-DBDI-MSI system to detect difenoconazole, leaves from difenoconazole-free tomato seedlings were selected first, using the same sample pre-treatment process. After that, 5 μL of difenoconazole solutions with different concentrations were pipetted onto their surfaces. Allow to air dry. Then, LA-DBDI-MS was used to analyze the difenoconazole-treated leaves. The difenoconazole content per unit area was calculated based on the concentration of the drop. Mass spectra from tomato leaves with different difenoconazole concentrations were also obtained, and as shown in Fig. 3(b), the MS signal intensity of difenoconazole increased linearly with the concentration of the difenoconazole solution pipetted onto tomato leaves (5 measurements per sample). In the range of 20–500 ng/μm^2, the equation for this calibration curve was $y = 22.7\ x + 64.6$ ($R^2 = 0.9874$) and the LOD was 6.2 ng/μm^2. Fig. 3(c) shows the MS signal of an aqueous solution of difenoconazole at a concentration of 100 ppm (signals at $m/z = 231$, 249, and 279 are peaks from plasticizers present in laboratory air). The strong signal at $m/z = 406$ represents the difenoconazole molecule. Signals at $m/z = 407$, 408, 409, and 410 present in Fig. 3(c) are isotopic peaks due to ^{37}Cl and ^{13}C. Fig. 3(d) shows a mass spectrum of a tomato leaf without difenoconazole. Signals at $m/z = 70$, 80, 90, 129, etc. are probably due to endogenous substances in the leaves themselves, but not from difenoconazole. We selected the characteristic peak of difenoconazole at $m/z = 406$ for MS imaging.

3.2. Studying Pesticide Translocation

The schematic in Fig. 4 shows the workflow for the study of the absorption and translocation behaviors of difenoconazole in tomato plants. In this study, difenoconazole was applied to the roots or leaves of tomato seedlings, respectively. After tomato seedlings were exposed to difenoconazole for a certain period of time, difenoconazole was absorbed by the roots or leaves and then translocated to other plant tissues. A target leaf was selected from the first branch of the plant for the case where pesticides were applied to the roots. Difenoconazole signals on these leaves were monitored by LA-DBDI-MSI. When tomato seedlings

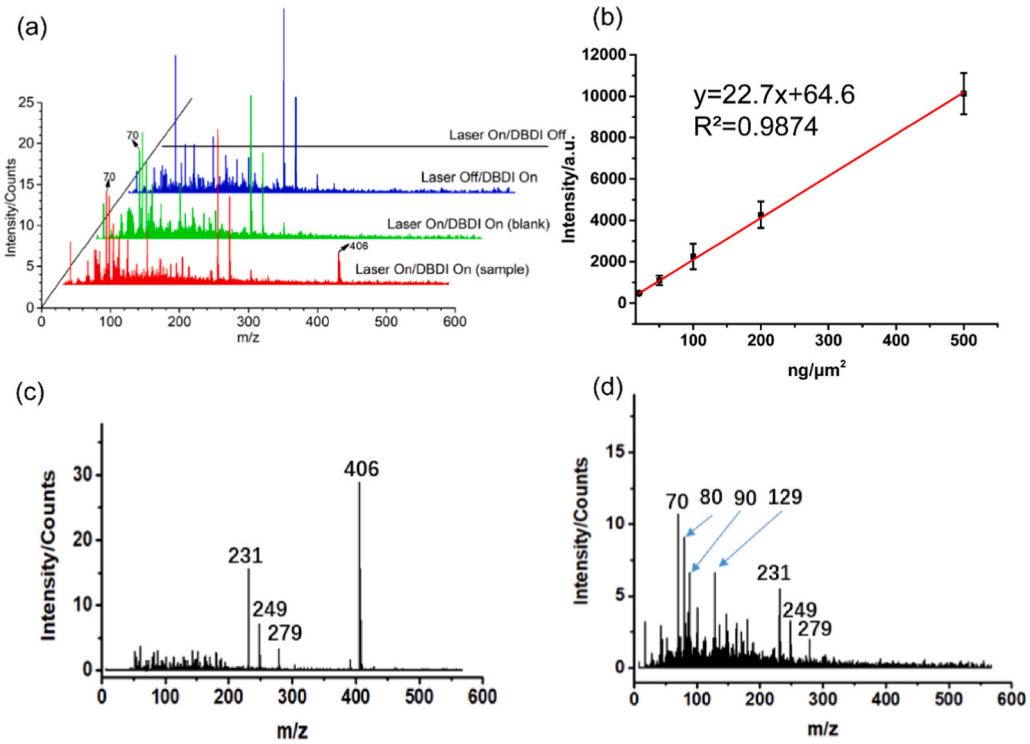

Fig. 3. (a) Mass spectra of difenoconazole on tomato leaves after 10 days of applying difenoconazole on the roots, obtained by LA-DBDI-MS. (b) Plot of the signal intensity of the mass spectral signal versus the amount of drug per unit area on the leaf, covering a range from 20 ng/μm^2 to 500 ng/μm^2. (c) MS signal of an aqueous solution of difenoconazole at a concentration of 100 ppm. (d) MS signal of tomato leaves without difenoconazole. *m/z* 231, 249, and 279 are plasticizers present in the laboratory air.

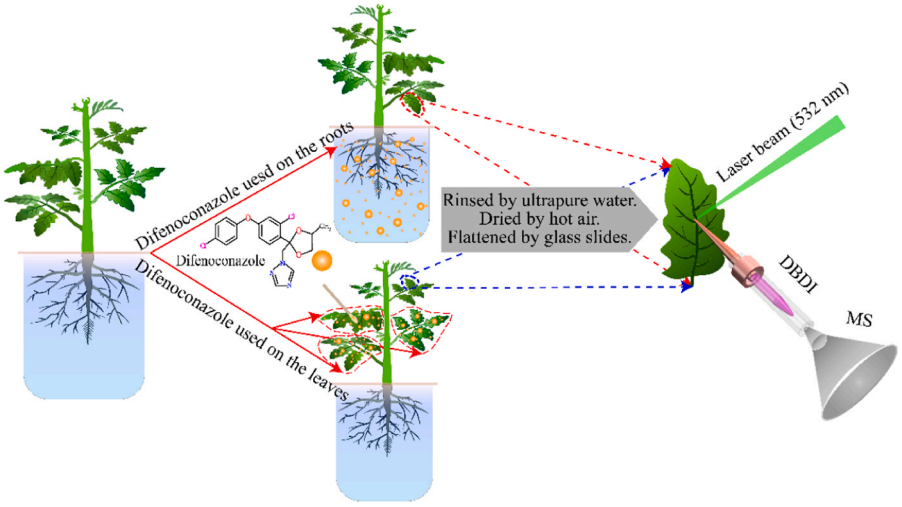

Fig. 4. Workflow for studying the absorption and translocation behaviors of difenoconazole in tomato plants.

were exposed to difenoconazole for six or ten days, a target leaf was taken, using the same treatment as described in the sample pretreatment process. Then, the distribution of difenoconazole on the leaf was obtained using LA-DBDI-MSI. Similarly, we studied the absorption and translocation behavior of difenoconazole for the case where pesticide was applied to the leaves. After tomato seedlings were exposed to difenoconazole for 6 or 10 days, the MSI of the distribution of difenoconazole on the target leaves that were not directly brushed with pesticides were obtained.

3.3. Spatiotemporal distribution of difenoconazole within tomato leaves

To study the absorption and translocation behaviors of difenoconazole in tomato seedlings, LA-DBDI-MSI was performed on treated tomato leaves after a simple sample pre-preparation for target tomato leaves. As shown in Fig. 5(b) and (c), 5 × 5 mm^2 (200 ×200 pixels) MS images were obtained after the roots had been exposed to difenoconazole solution for 6 days. By comparing an optical image of the leaf after laser ablation (Fig. 5(a)) with the MS images (Fig. 5(b), (c)) obtained, the MS images matched well with the optical image. This means that the MSI represents a faithful mapping of the distribution of difenoconazole in tomato leaves, and is not disturbed by artifacts. In Fig. 5(c), the intensity

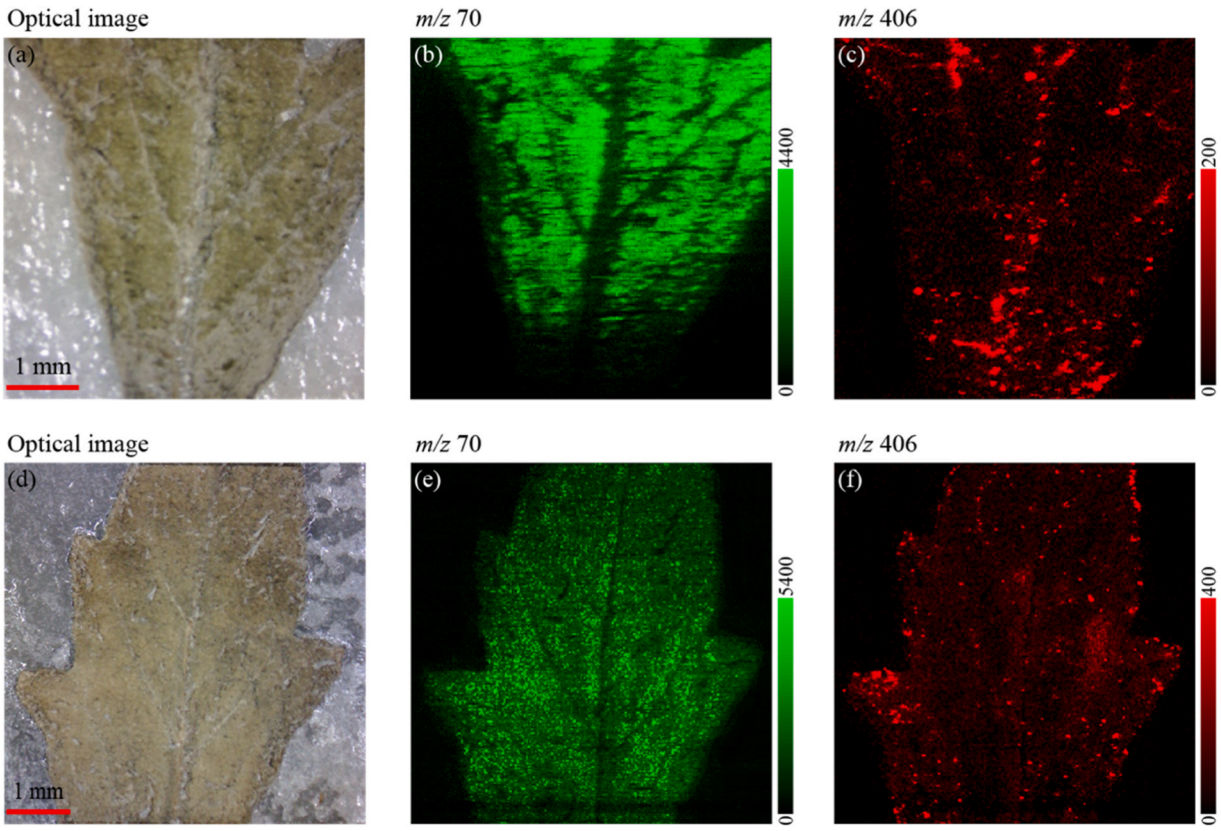

Fig. 5. (a) Optical microscopy image of tomato leaves, after roots exposed to pesticides for 6 days. (b-c) LA-DBDI-MSI of different selected ions at (b) $m/z = 70$, (c) $m/z = 406$. (d) Optical microscopy image of tomato leaves, after roots exposed to pesticides for 10 days. (e-f) LA-DBDI-MSI of different selected ions at (e) $m/z = 70$, (f) $m/z = 406$.

of MS signal of difenoconazole on tomato leaves was weak. By comparing Fig. 5(a) with Fig. 5(c), we can draw a preliminary conclusion that difenoconazole is mainly distributed in tomato leaf midrib and side veins, and almost absent in the mesophyll. This indicates that difenoconazole can be absorbed by the roots and translocated to leaves within 6 days of exposure to pesticides.

When the time of pesticide exposure was extended to 10 days, we also obtained 6×6 mm^2 (240 × 240 pixels) MS images on target leaves, see Fig. 5(e) and (f). The MS images of $m/z = 406$ in Fig. 5(f) clearly revealed the distribution of difenoconazole on the target leaf. In this case, difenoconazole is more evenly distributed throughout the tomato leaves. This demonstrates that with the extension of the time of exposing the roots to the pesticide, the difenoconazole molecules are gradually transported to the whole leaf. Blank experiments with tomato seedlings that were not exposed to difenoconazole were also performed, after 6 days and 10 days cultivation, but no signals at $m/z = 406$ were detected on tomato leaves.

After that, we investigated the absorption and translocation behaviors of difenoconazole on tomato seedlings when the leaves were exposed to difenoconazole solution. In Fig. 6(b), (c), (e), and (f), MSI data in a region of interest on a target leaf were obtained. In Fig. 6(c), the distribution of difenoconazole clearly mapped the tree-like structure of leaf midrib and side veins after 6 days of leaf exposure to pesticides, i.e., the distribution of difenoconazole co-locates with the leaf veins. At the same time, the MS signal intensity of difenoconazole on the leaf midrib was higher than that on the leaf side veins and mesophyll; the farther away from the leaf veins, the weaker the signal intensity of $m/z = 406$. These results confirms that pesticide can be absorbed by tomato leaves and be transferred to other leaves. As the time of leaf exposed to pesticide was extended to 10 days, difenoconazole was distributed evenly over the entire leaf. We could no longer find the geometrical arrangement of leaf veins in Fig. 6(f). Therefore, we can conclude that with the extension of exposure time of leaves to pesticides, difenoconazole can be continually absorbed by leaves, and gradually translocated from the midrib to the side vein, then to the mesophyll, and will finally be distributed throughout the leaf [42].

Overall, our results show that pesticides can be absorbed into plants either via the roots or via leaves, and then be transported to other plant tissues. With increasing exposure time, pesticide becomes more evenly distributed in the whole leaf, which is helpful for prevention of pests and fungi.

In addition, when processing the imaging data, we found other mass spectral signals (e.g., nominal $m/z = 70$, 80, 86, 90, 98, 129,.), which were always present with a different spatial distribution than that of $m/z = 406$, see Fig. 5(b), (e) and 6 (b), (e). No matter how the pesticide was applied or how long the exposure time was, $m/z = 70$, the most prominent of these signals, was only found in the mesophyll, not in the veins. At the same time, this signal was also detected in tomato leaves in the blank experiment. Thus, these signals must represent compounds that are unrelated to the pesticide, but derived from an endogenous substance in tomato leaves. We spent significant efforts to try to identify some of the endogeneous signals from the tomato leaves, using extraction with acetonitrile followed by LC-ESI MS/MS analysis. Unfortunately, the most prominent signals, notably $m/z = 70$, could not be detected in the extract, probably due to the polarity of the solvent and the different ionization method used (ESI; DBDI could not be interfaced with LC and MS/MS). We surmise the $m/z = 70$ peak to be a fragment from a hitherto unidentified endogeneous metabolite present in the tomato leaves.

Based on the MSI results, we propose a possible mechanism of absorption and translocation of difenoconazole in tomato seedlings, as shown in Fig. 7. Difenoconazole can be absorbed into plants first by

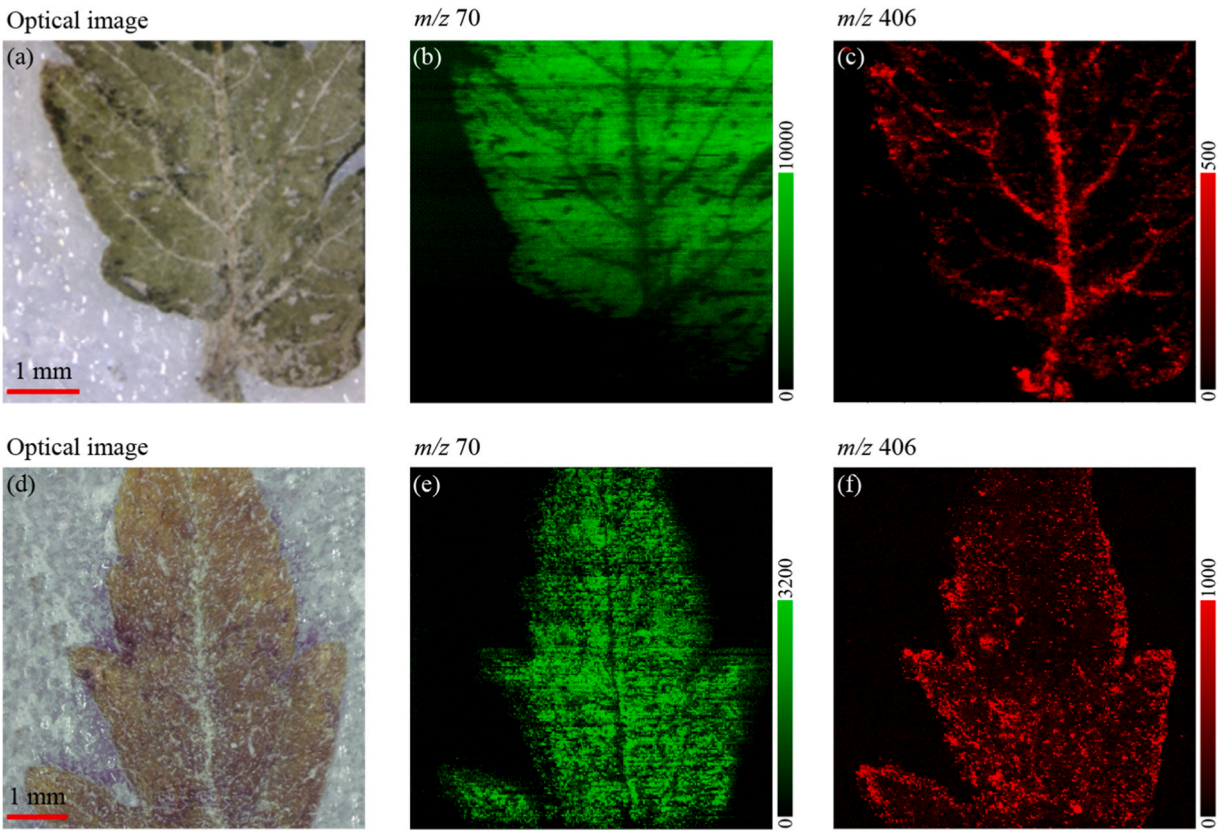

Fig. 6. (a) Optical microscopy image of target tomato leaves (without directly bushed pesticides on it) after other tomato leaves exposed to pesticides for 6 days. (b-c) LA-DBDI-MSI of different selected ions at (b) $m/z = 70$, (c) $m/z = 406$. (d) Optical microscopy image of target tomato leaves (without directly bushed pesticides on it) after other tomato leaves exposed to pesticides for 10 days. (e-f) LA-DBDI-MSI of different selected ions at (e) $m/z = 70$, (f) $m/z = 406$.

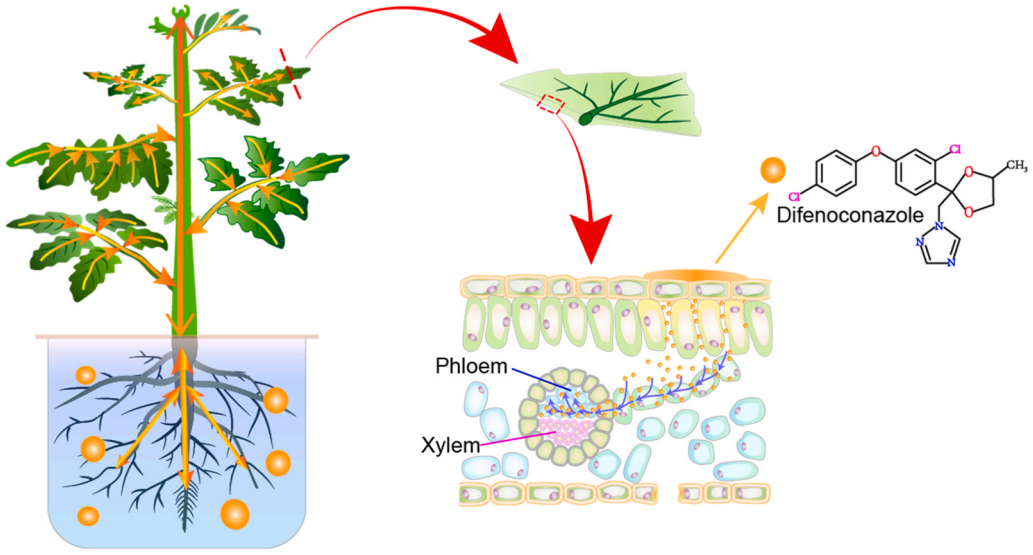

Fig. 7. Absorption and translocation mechanism for systemic pesticides difenoconazole are revealed by LA-DBDI MSI. (a) Schematic of the translocation processes of pesticides throughout the entire plant vascular systems, including roots, stems, and leaves. (b) Absorption processes of difenoconazole from leaf or roots to the phloem translocation system.

tomato leaves or roots, and then translocate to leaves through vascular tissue. When the pesticide reaches the leaf, the pesticide will be transported further through the leaf midrib and the side vein to the mesophyll. Moreover, leaf veins are composed of xylem and phloem. The phloem can actively transport organic nutrients (e.g., amino acids, sugars) from top to bottom, and the xylem transports water and inorganic salts passively from bottom to top. In the schematic, difenoconazole could be absorbed by the leaf surface, then concentrated on the leaf veins, and transported from the petiole to the stalk via the phloem from top to bottom. After that, the pesticide is transported to the stalks are translocated from bottom to top along the stem-petiole-vein-mesophyll to the upper leaves. This indicates that difenoconazole is

mainly transported through the phloem and the uptake and translocation of difenoconazole are an active process of the plant itself. Of course, pesticide can also be absorbed by roots and then transported from bottom to top along the root-stem-leaf.

4. Conclusions

In this paper, we combined laser ablation, DBDI post-ionization, and atmospheric pressure mass spectrometry for constructing a LA-DBDI-MSI system, to achieve high-throughput MS imaging of biological samples under atmospheric pressure. LA-DBDI MSI was performed to study the absorption and translocation behavior of pesticides in tomato seedlings. MS images of tomato leaves under different ways of applying pesticides and different pesticide exposure times were obtained. After 6 days of exposing either the roots or leaves to a pesticide, the spatial distribution of difenoconazole on tomato leaves could be obtained, and was found to co-localize with the veins. With increasing pesticide exposure time, difenoconazole is gradually transported from the veins to the mesophyll, and finally evenly distributed throughout the leaves. At the same time, we also obtained the distribution of $m/z = 70$ on tomato leaves. Due to its characteristic that it is only distributed on the mesophyll, we speculate that it may be derived from chlorophyll. This method successfully allows visualization of pesticides without the need for any derivatization in tomato plants, and allows conclusions about the translocation process of systemic pesticides in plants to be drawn, which may provide guidance for the use of pesticides and help reduce pesticide pollution.

CRediT authorship contribution statement

Renato Zenobi: Writing – review & editing, Supervision, Project administration, Methodology, Funding acquisition, Conceptualization. **Zhouyi Xu:** Investigation. **Xiaokang Guan:** Investigation, Formal analysis. **Qiao Lu:** Writing – review & editing, Writing – original draft, Methodology, Investigation, Conceptualization. **Xue You:** Writing – original draft, Visualization, Validation, Methodology, Investigation, Formal analysis, Data curation.

Declaration of Competing Interest

The authors declare that they have no known competing financial interests or personal relationships that could have appeared to influence the work reported in this paper.

Data availability

Data will be made available on request.

Acknowledgements

This work was financially supported by the National Natural Science Foundation of China (grants no. 21874111 and no. 22304050) and the Hubei Provincial Natural Science Foundation of China (no. 2023AFB271).

References

[1] M. Wojciechowska, P. Stepnowski, M. Golebiowski, The use of insecticides to control insect pests, Invertebr. Surviv. J. 13 (2016) 210–220.
[2] K. Grossmann, Auxin herbicides: current status of mechanism and mode of action, Pest Manag Sci. 66 (2010) 113–120.
[3] K. Jiang, T. Asami, Chemical regulators of plant hormones and their applications in basic research and agriculture, Biosci. Biotechnol. Biochem. 82 (2018) 1265–1300.
[4] M.H. Zhang, M.R. Zeiss, S. Geng, Agricultural pesticide use and food safety: California's model, J. Integr. Agric. 14 (2015) 2340–2357.
[5] Y.X. Liu, L. Lonappan, S.K. Brar, S.M. Yang, Impact of biochar amendment in agricultural soils on the sorption, desorption, and degradation of pesticides: a review, Sci. Total Environ. 645 (2018) 60–70.
[6] J. Potapowicz, D. Lambropoulou, C. Nannou, K. Koziol, Z. Polkowska, Occurrences, sources, and transport of organochlorine pesticides in the aquatic environment of Antarctica, Sci. Total Environ. 735 (2020) 139475.
[7] P. Nicolopoulou-Stamati, S. Maipas, C. Kotampasi, P. Stamatis, L. Hens, Chemical pesticides and human health: the urgent need for a new concept in agriculture, Front. Public Health 4 (2016) 148.
[8] V.P. Kalyabina, E.N. Esimbekova, K.V. Kopylova, V.A. Kratasyuk, Pesticides: formulants, distribution pathways and effects on human health - a review, Toxicol. Rep. 8 (2021) 1179–1192.
[9] D. Pimentel, Amounts of pesticides reaching target pests - environmental impacts and ethics, J. Agric. Environ. Ethics 8 (1995) 17–29.
[10] D. Tilman, K.G. Cassman, P.A. Matson, R. Naylor, S. Polasky, Agricultural sustainability and intensive production practices, Nature 418 (2002) 671–677.
[11] M. Rundlof, G.K.S. Andersson, R. Bommarco, I. Fries, V. Hederstrom, L. Herbertsson, et al., Seed coating with a neonicotinoid insecticide negatively affects wild bees, Nature 521 (2015) 77–U162.
[12] T.M. Abdelrahman, X. Qin, D. Li, I.A. Senosy, M. Mmby, H. Wan, et al., Pectinase-responsive carriers based on mesoporous silica nanoparticles for improving the translocation and fungicidal activity of prochloraz in rice plants, Chem. Eng. J. 404 (2021) 125440.
[13] Z.W. Lei, J. Wang, G.L. Mao, Y.J. Wen, Y.X. Tian, H.W. Wu, et al., Glucose positions affect the phloem mobility of glucose-fipronil conjugates, J. Agric. Food Chem. 62 (2014) 6065–6071.
[14] C. Ju, H.C. Zhang, S.J. Yao, S.X. Dong, D.T. Cao, F.Y. Wang, et al., Uptake, Translocation, and subcellular distribution of Azoxystrobin in wheat plant (Triticum aestivum L, J. Agric. Food Chem. 67 (2019) 6691–6699.
[15] C. Ju, H.C. Zhang, R.L. Wu, S.X. Dong, S.J. Yao, F.Y. Wang, et al., Upward translocation of acetochlor and atrazine in wheat plants depends on their distribution in roots, Sci. Total Environ. 703 (2020) 135636.
[16] C. Ju, S.X. Dong, H.C. Zhang, S.J. Yao, F.Y. Wang, D.T. Cao, et al., Subcellular distribution governing accumulation and translocation of pesticides in wheat (Triticum aestivum L.), Chemosphere 248 (2020) 126064.
[17] M.Q. Zhu, X. Ou, J. Tang, T.Z. Shi, X. Ma, Y. Wang, et al., Uptake, distribution and translocation of imidacloprid-loaded fluorescence double hollow shell mesoporous silica nanoparticles and metabolism of imidacloprid in pakchoi, Sci. Total Environ. 787 (2021) 147578.
[18] C. Zhang, J.M. Xue, D.M. Cheng, Y. Feng, Y.W. Liu, H.M. Aly, et al., Uptake, translocation and distribution of three veterinary antibiotics in Zea mays L, Environ. Pollut. 250 (2019) 47–57.
[19] W.K. Chu, M.H. Wong, J. Zhang, Accumulation, distribution and transformation of DDT and PCBs by Phragmites australis and Oryza sativa L.: I. Whole plant study, Environ. Geochem. Health 28 (2006) 159–168.
[20] M. Kubicki, M. Lamshoft, A. Lagojda, M. Spiteller, Metabolism and spatial distribution of metalaxyl in tomato plants grown under hydroponic conditions, Chemosphere 218 (2019) 36–41.
[21] H. Schrey, F.J. Muller, P. Harz, Z. Rupcic, M. Stadler, P. Spiteller, Nematicidal anthranilic acid derivatives from Laccaria species, Phytochemistry 160 (2019) 85–91.
[22] M. Kubicki, G. Giannakopoulos, M. Lamshoft, J. Dittgen, Spatially resolved investigation of herbicide-safener interaction in Maize (Zea mays L.) by MALDI-imaging mass spectrometry, J. Agric. Food Chem. 70 (2022) 6368–6376.
[23] D.A. Kleier, F.C. Hsu, Phloem mobility of xenobiotics.7. The design of phloem systemic pesticides, Weed Sci. 44 (1996) 749–756.
[24] M.M. Tong, W.J. Gao, W.T. Jiao, J. Zhou, Y.Y. Li, L.L. He, et al., Uptake, translocation, metabolism, and distribution of glyphosate in nontarget tea plant (Camellia sinensis L, J. Agric. Food Chem. 65 (2017) 7638–7646.
[25] L. Castle, Determination of acrylamide monomer in mushrooms grown on polyacrylamide-gel, J. Agric. Food Chem. 41 (1993) 1261–1263.
[26] F. Chowdhury, G. Langenkamper, M. Grote, Studies on uptake and distribution of antibiotics in red cabbage, J. Verbrauch. Lebensm. J. Consum. Prot. Food Saf. 11 (2016) 61–69.
[27] A. Macherius, T. Eggen, W.G. Lorenz, T. Reemtsma, U. Winkler, M. Moeder, Uptake of galaxolide, tonalide, and triclosan by carrot, barley, and meadow fescue plants, J. Agric. Food Chem. 60 (2012) 7785–7791.
[28] H. Zhang, J. Jiang, N. Li, M. Li, Y. Wang, J. He, et al., Surface Desorption Dielectric-Barrier Discharge Ionization Mass Spectrometry, Anal. Chem. 89 (2017) 7333–7339.
[29] R.Y. Hou, Z.Y. Zhang, S. Pang, T.X. Yang, J.M. Clark, L.L. He, Alteration of the nonsystemic behavior of the pesticide ferbam on tea leaves by engineered gold nanoparticles, Environ. Sci. Technol. 50 (2016) 6216–6223.
[30] F. Kreye, G. Hamm, Y. Karrout, R. Legouffe, D. Bonnel, F. Siepmann, et al., MALDI-TOF MS imaging of controlled release implants, J. Control Release 161 (2012) 98–108.
[31] D. Pietkiewicz, A. Horala, S. Plewa, P. Jasinski, E. Nowak-Markwitz, Z.J. Kokot, et al., MALDI-MSI-a step forward in overcoming the diagnostic challenges in ovarian tumors, Int. J. Environ. Res. Public Health 17 (2020).
[32] A. Moreno-Pedraza, I. Rosas-Roman, N.S. Garcia-Rojas, H. Guillen-Alonso, C. Ovando-Vazquez, D. Diaz-Ramirez, et al., Elucidating the distribution of plant metabolites from native tissues with laser desorption low-temperature plasma mass spectrometry imaging, Anal. Chem. 91 (2019) 2734–2743.
[33] B. Li, J.Y. Ge, W. Liu, D.J. Hu, P. Li, Unveiling spatial metabolome of Paeonia suffruticosa and Paeonia lactiflora roots using MALDI MS imaging, N. Phytol. 231 (2021) 892–902.
[34] M.K. Passarelli, A. Pirkl, R. Moellers, D. Grinfeld, F. Kollmer, R. Havelund, et al., The 3D OrbiSIMS-label-free metabolic imaging with subcellular lateral resolution and high mass-resolving power, Nat. Methods 14 (2017) 1175–1183.

[35] Z. Takats, J.M. Wiseman, B. Gologan, R.G. Cooks, Mass spectrometry sampling under ambient conditions with desorption electrospray ionization, Science 306 (2004) 471–473.
[36] M. Kompauer, S. Heiles, B. Spengler, Atmospheric pressure MALDI mass spectrometry imaging of tissues and cells at 1.4-mu m lateral resolution, Nat. Methods 14 (2017) 90–96.
[37] S.A. Stopka, E.A. Wood, R. Khattar, B.J. Agtuca, W.M. Abdelmoula, N.Y.R. Agar, et al., High-throughput analysis of tissue-embedded single cells by mass spectrometry with bimodal imaging and object recognition, Anal. Chem. 93 (2021) 9677–9687.
[38] J.Y. Kim, E.S. Seo, H. Kim, J.-W. Park, D.-K. Lim, D.W. Moon, Atmospheric pressure mass spectrometric imaging of live hippocampal tissue slices with subcellular spatial resolution, Nat. Commun. 8 (2017) 2113.
[39] Q. Lu, Z. Xu, X. You, S. Ma, R. Zenobi, Atmospheric pressure mass spectrometry imaging using laser ablation, followed by dielectric barrier discharge ionization, Anal. Chem. 93 (2021) 6232–6238.
[40] M.F. Mirabelli, E. Gionfriddo, J. Pawliszyn, R. Zenobi, A quantitative approach for pesticide analysis in grape juice by direct interfacing of a matrix compatible SPME phase to dielectric barrier discharge ionization-mass spectrometry, Analyst 143 (2018) 891–899.
[41] A. Schutz, S. Brandt, S. Liedtke, D. Foest, U. Marggraf, J. Franzke, Dielectric barrier discharge ionization of perfluorinated compounds, Anal. Chem. 87 (2015) 11415–11419.
[42] F. Sicbaldi, G.A. Sacchi, M. Trevisan, A.A.M. DelRe, Root uptake and xylem translocation of pesticides from different chemical classes, Pestic. Sci. 50 (1997) 111–119.

Xue You was a M.Sc. student at the Department of Chemistry and the MOE Key Laboratory of Spectrochemical Analysis & Instrumentation, College of Chemistry and Chemical Engineering, Xiamen University, China. He graduated in 2022, and is now working for private industry.

Qiao Lu was a Ph.D. student at the Department of Chemistry and the MOE Key Laboratory of Spectrochemical Analysis & Instrumentation, College of Chemistry and Chemical Engineering, Xiamen University, China. He graduated in 2022, and is now on the faculty of the Department of Laboratory Medicine, Taihe Hospital, Hubei University of Medicine, in Shiyan, China.

Xiaokang Guan, is a Ph.D. student at the Department of Chemistry and the MOE Key Laboratory of Spectrochemical Analysis & Instrumentation, College of Chemistry and Chemical Engineering, Xiamen University, China.

Zhouyi Xu was a postdoctoral scholar at the Department of Chemistry and the MOE Key Laboratory of Spectrochemical Analysis & Instrumentation, College of Chemistry and Chemical Engineering, Xiamen University, China. He is now an assistant professor at Xiamen University.

Renato Zenobi is Professor of Analytical Chemistry at the Department of Chemistry and Applied Biosciences, ETH Zurich in Switzerland. He also has long-term visiting professor appointment at the Department of Chemistry and the MOE Key Laboratory of Spectrochemical Analysis & Instrumentation, College of Chemistry and Chemical Engineering, Xiamen University, China.